

Benefits

- High precision op amp without the need of calibration
- Accuracy virtually unaffected by temperature change

Applications

- Wearable
- Fitness and healthcare
- Medical instrumentation

Description

The OA1ZHA, OA2ZHA, OA4ZHA series of low power, high precision op amp, offer very low input offset voltages with virtually zero drift.

OA1ZHA, OA2ZHA, OA4ZHA are respectively the single, dual and quad operational amplifier versions, with pinout compatible with industry standards.

The OA1ZHA, OA2ZHA, OA4ZHA series offers rail-to-rail input and output, excellent speed/power consumption ratio, and 400 kHz gain bandwidth product, while consuming less than 40 μA at 5 V. All devices also feature an ultra-low input bias current.

The OA1ZHA, OA2ZHA, OA4ZHA family is the ideal choice for wearable, fitness and healthcare applications.

Features

- Very high accuracy and stability: offset voltage 5 μV max at 25°C, 8 μV over full temperature range (-40°C to 125°C)
- Rail-to-rail input and output
- Low supply voltage: 1.8 - 5.5 V
- Low power consumption: 40 μA max. at 5 V
- Gain bandwidth product: 400 kHz
- High tolerance to ESD: 4 kV HBM
- Extended temperature range: -40 to +125°C
- Micro-packages: SC70-5, DFN8 2x2, and QFN16 3x3

Table 1. Device summary

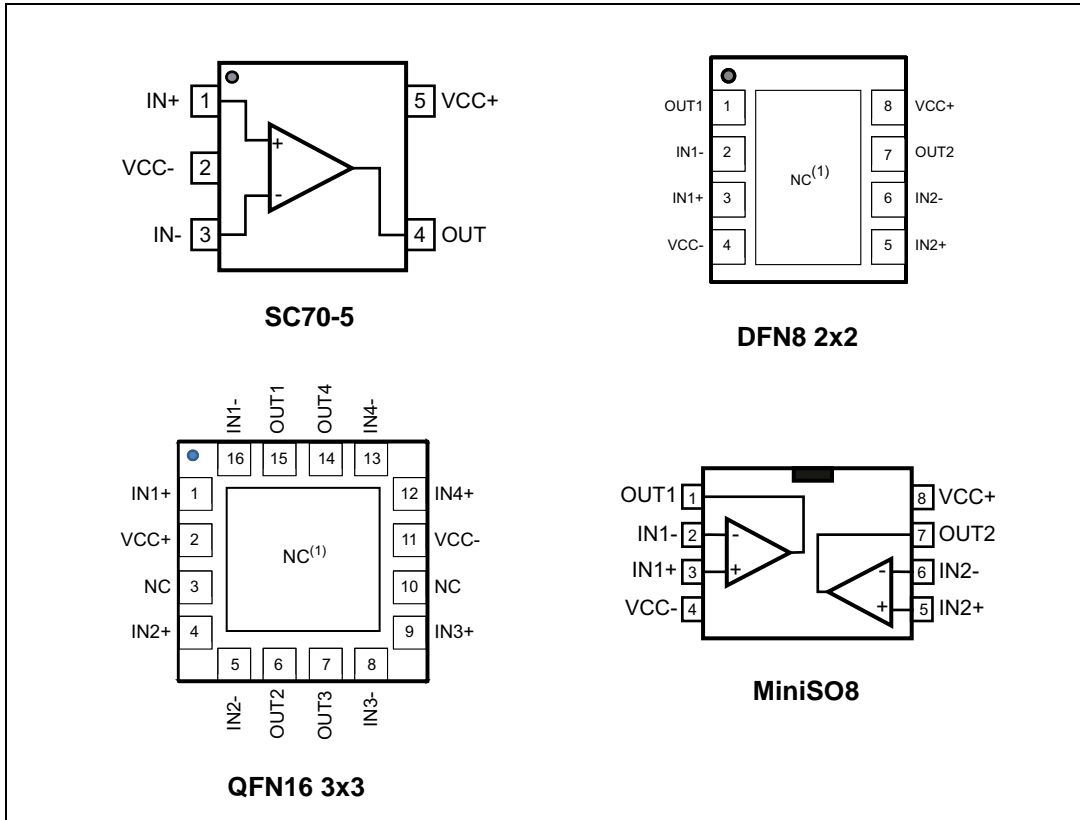
Order code	Temperature range	Package	Packaging	Marking
OA1ZHA22C	-40 to +125 °C	SC70-5	Tape and reel	K44
OA2ZHA22Q		DFN8 2x2		K33
OA2ZHA34S		MiniSO8		K143
OA4ZHA33Q		QFN16 3x3		K193

Contents

- 1 Package pin connections 3**
- 2 Absolute maximum ratings and operating conditions 4**
- 3 Electrical characteristics 5**
- 4 Application information 17**
 - 4.1 Operation theory 17
 - 4.1.1 Time domain 17
 - 4.1.2 Frequency domain 18
 - 4.2 Operating voltages 19
 - 4.3 Input pin voltage ranges 19
 - 4.4 Rail-to-rail input 19
 - 4.5 Input offset voltage drift over temperature 20
 - 4.6 Rail-to-rail output 20
 - 4.7 Capacitive load 20
 - 4.8 PCB layout recommendations 21
 - 4.9 Optimized application recommendation 22
 - 4.10 EMI rejection ration (EMIRR) 22
 - 4.11 Application examples 23
 - 4.11.1 Oxygen sensor 23
 - 4.11.2 Precision instrumentation amplifier 24
 - 4.11.3 Low-side current sensing 25
- 5 Package information 26**
 - 5.1 SC70-5 package information 27
 - 5.2 DFN8 2x2 package information 28
 - 5.3 MiniSO8 package information 30
 - 5.4 QFN16 3x3 package information 31
- 6 Revision history 33**

1 Package pin connections

Figure 1. Pin connections for each package (top view)



1. The exposed pads of the DFN8 2x2 and the QFN16 3x3 can be connected to VCC- or left floating.

2 Absolute maximum ratings and operating conditions

Table 2. Absolute maximum ratings (AMR)

Symbol	Parameter	Value	Unit
V_{CC}	Supply voltage ⁽¹⁾	6	V
V_{id}	Differential input voltage ⁽²⁾	$\pm V_{CC}$	
V_{in}	Input voltage ⁽³⁾	$V_{CC-} - 0.2$ to $V_{CC+} + 0.2$	
I_{in}	Input current ⁽⁴⁾	10	mA
T_{stg}	Storage temperature	-65 to +150	°C
R_{thja}	Thermal resistance junction-to-ambient ⁽⁵⁾⁽⁶⁾		°C/W
	SC70-5	205	
	DFN8 2x2	57	
	MiniSO8	190	
	QFN16 3x3	39	
T_j	Maximum junction temperature	150	°C
ESD	HBM: human body model, OA1ZHA only ⁽⁷⁾	4	kV
	MM: machine model, OA1ZHA only ⁽⁸⁾	300	V
	CDM: charged device model	1.5	kV
	CDM: charged device model, QFN16 3x3	TBD	
	Latch-up immunity	200	mA

1. All voltage values, except differential voltage, are with respect to network ground terminal.
2. The differential voltage is the non-inverting input terminal with respect to the inverting input terminal.
3. $V_{CC-} - V_{in}$ must not exceed 6 V, V_{in} must not exceed 6 V.
4. Input current must be limited by a resistor in series with the inputs.
5. Short-circuits can cause excessive heating and destructive dissipation.
6. R_{th} are typical values.
7. Human body model: 100 pF discharged through a 1.5 kΩ resistor between two pins of the device, done for all couples of pin combinations with other pins floating.
8. Machine model: a 200 pF cap is charged to the specified voltage, then discharged directly between two pins of the device with no external series resistor (internal resistor < 5 Ω), done for all couples of pin combinations with other pins floating.

Table 3. Operating conditions

Symbol	Parameter	Value	Unit
V_{CC}	Supply voltage	1.8 to 5.5	V
V_{icm}	Common mode input voltage range	$V_{CC-} - 0.1$ to $V_{CC+} + 0.1$	
T_{oper}	Operating free air temperature range	-40 to +125	°C

3 Electrical characteristics

$V_{CC+} = 1.8\text{ V}$ with $V_{CC-} = 0\text{ V}$, $V_{icm} = V_{CC}/2$, $T = 25\text{ °C}$, and $R_L = 10\text{ k}\Omega$ connected to $V_{CC}/2$ (unless otherwise specified)

Table 4. Electrical characteristics

Symbol	Parameter	Conditions	Min.	Typ.	Max.	Unit
DC performance						
V_{io}	Input offset voltage	$T = 25\text{ °C}$		1	5	μV
		$-40\text{ °C} < T < 125\text{ °C}$			8	
$\Delta V_{io}/\Delta T$	Input offset voltage drift ⁽¹⁾	$-40\text{ °C} < T < 125\text{ °C}$		10	30	$\text{nV}/\text{°C}$
I_{ib}	Input bias current ($V_{out} = V_{CC}/2$)	$T = 25\text{ °C}$		50	200 ⁽²⁾	pA
		$-40\text{ °C} < T < 125\text{ °C}$			300 ⁽²⁾	
I_{io}	Input offset current ($V_{out} = V_{CC}/2$)	$T = 25\text{ °C}$		100	400 ⁽²⁾	pA
		$-40\text{ °C} < T < 125\text{ °C}$			600 ⁽²⁾	
CMR	Common mode rejection ratio 20 log ($\Delta V_{icm}/\Delta V_{io}$), $V_{ic} = 0\text{ V}$ to V_{CC} , $V_{out} = V_{CC}/2$, $R_L > 1\text{ M}\Omega$	$T = 25\text{ °C}$	110	122		dB
		$-40\text{ °C} < T < 125\text{ °C}$	110			
A_{vd}	Large signal voltage gain $V_{out} = 0.5\text{ V}$ to $(V_{CC} - 0.5\text{ V})$	$T = 25\text{ °C}$	118	135		dB
		$-40\text{ °C} < T < 125\text{ °C}$	110			
V_{OH}	High level output voltage	$T = 25\text{ °C}$			30	mV
		$-40\text{ °C} < T < 125\text{ °C}$			70	
V_{OL}	Low level output voltage	$T = 25\text{ °C}$			30	mV
		$-40\text{ °C} < T < 125\text{ °C}$			70	
I_{out}	I_{sink} ($V_{out} = V_{CC}$)	$T = 25\text{ °C}$	7	8		mA
		$-40\text{ °C} < T < 125\text{ °C}$	6			
	I_{source} ($V_{out} = 0\text{ V}$)	$T = 25\text{ °C}$	5	7		
		$-40\text{ °C} < T < 125\text{ °C}$	4			
I_{CC}	Supply current (per channel, $V_{out} = V_{CC}/2$, $R_L > 1\text{ M}\Omega$)	$T = 25\text{ °C}$		28	40	μA
		$-40\text{ °C} < T < 125\text{ °C}$			40	
AC performance						
GBP	Gain bandwidth product	$R_L = 10\text{ k}\Omega$, $C_L = 100\text{ pF}$		400		kHz
F_u	Unity gain frequency			300		
Φ_m	Phase margin			55		degrees
G_m	Gain margin			17		dB
SR	Slew rate ⁽³⁾			0.17		$\text{V}/\mu\text{s}$
t_s	Settling time		To 0.1%, $V_{in} = 1\text{ Vp-p}$, $R_L = 10\text{ k}\Omega$, $C_L = 100\text{ pF}$		50	

Table 4. Electrical characteristics (continued)

Symbol	Parameter	Conditions	Min.	Typ.	Max.	Unit
e_n	Equivalent input noise voltage	f = 1 kHz f = 10 kHz		60 60		$\frac{nV}{\sqrt{Hz}}$
C_s	Channel separation	f = 100 Hz		120		dB
t_{init}	Initialization time	T = 25 °C -40 °C < T < 125 °C		50 100		μs

1. See [Section 4.5: Input offset voltage drift over temperature](#). Input offset measurements are performed on x100 gain configuration. The amplifiers and the gain setting resistors are at the same temperature.
2. Guaranteed by design.
3. Slew rate value is calculated as the average between positive and negative slew rates.

$V_{CC+} = 3.3\text{ V}$ with $V_{CC-} = 0\text{ V}$, $V_{icm} = V_{CC}/2$, $T = 25\text{ °C}$, and $R_L = 10\text{ k}\Omega$ connected to $V_{CC}/2$ (unless otherwise specified)

Table 5. Electrical characteristics

Symbol	Parameter	Conditions	Min.	Typ.	Max.	Unit
DC performance						
V_{io}	Input offset voltage	$T = 25\text{ °C}$		1	5	μV
		$-40\text{ °C} < T < 125\text{ °C}$			8	
$\Delta V_{io}/\Delta T$	Input offset voltage drift ⁽¹⁾	$-40\text{ °C} < T < 125\text{ °C}$		10	30	$\text{nV}/\text{°C}$
I_{ib}	Input bias current ($V_{out} = V_{CC}/2$)	$T = 25\text{ °C}$		60	200 ⁽²⁾	pA
		$-40\text{ °C} < T < 125\text{ °C}$			300 ⁽²⁾	
I_{io}	Input offset current ($V_{out} = V_{CC}/2$)	$T = 25\text{ °C}$		120	400 ⁽²⁾	pA
		$-40\text{ °C} < T < 125\text{ °C}$			600 ⁽²⁾	
CMR	Common mode rejection ratio $20 \log (\Delta V_{icm}/\Delta V_{io})$ $V_{ic} = 0\text{ V}$ to V_{CC} , $V_{out} = V_{CC}/2$ $R_L > 1\text{ M}\Omega$	$T = 25\text{ °C}$	115	128		dB
		$-40\text{ °C} < T < 125\text{ °C}$	115			
A_{vd}	Large signal voltage gain $V_{out} = 0.5\text{ V}$ to $(V_{CC} - 0.5\text{ V})$	$T = 25\text{ °C}$	118	135		dB
		$-40\text{ °C} < T < 125\text{ °C}$	110			
V_{OH}	High level output voltage	$T = 25\text{ °C}$			30	mV
		$-40\text{ °C} < T < 125\text{ °C}$			70	
V_{OL}	Low level output voltage	$T = 25\text{ °C}$			30	mV
		$-40\text{ °C} < T < 125\text{ °C}$			70	
I_{out}	I_{sink} ($V_{out} = V_{CC}$)	$T = 25\text{ °C}$	15	18		mA
		$-40\text{ °C} < T < 125\text{ °C}$	12			
	I_{source} ($V_{out} = 0\text{ V}$)	$T = 25\text{ °C}$	14	16		
		$-40\text{ °C} < T < 125\text{ °C}$	10			
I_{CC}	Supply current (per channel, $V_{out} = V_{CC}/2$, $R_L > 1\text{ M}\Omega$)	$T = 25\text{ °C}$		29	40	μA
		$-40\text{ °C} < T < 125\text{ °C}$			40	
AC performance						
GBP	Gain bandwidth product	$R_L = 10\text{ k}\Omega$, $C_L = 100\text{ pF}$		400		kHz
F_u	Unity gain frequency			300		
Φ_m	Phase margin			56		degrees
G_m	Gain margin			19		dB
SR	Slew rate ⁽³⁾			0.19		$\text{V}/\mu\text{s}$
t_s	Settling time		To 0.1%, $V_{in} = 1\text{ Vp-p}$, $R_L = 10\text{ k}\Omega$, $C_L = 100\text{ pF}$		50	

Table 5. Electrical characteristics (continued)

Symbol	Parameter	Conditions	Min.	Typ.	Max.	Unit
e_n	Equivalent input noise voltage	f = 1 kHz f = 10 kHz		40 40		$\frac{nV}{\sqrt{Hz}}$
C_s	Channel separation	f = 100 Hz		120		dB
t_{init}	Initialization time	T = 25 °C		50		μs
		-40 °C < T < 125 °C		100		

1. See [Section 4.5: Input offset voltage drift over temperature](#). Input offset measurements are performed on x100 gain configuration. The amplifiers and the gain setting resistors are at the same temperature.
2. Guaranteed by design.
3. Slew rate value is calculated as the average between positive and negative slew rates.

$V_{CC+} = 5\text{ V}$ with $V_{CC-} = 0\text{ V}$, $V_{icm} = V_{CC}/2$, $T = 25\text{ °C}$, and $R_L = 10\text{ k}\Omega$ connected to $V_{CC}/2$ (unless otherwise specified)

Table 6. Electrical characteristics

Symbol	Parameter	Conditions	Min.	Typ.	Max.	Unit
DC performance						
V_{io}	Input offset voltage	$T = 25\text{ °C}$		1	5	μV
		$-40\text{ °C} < T < 125\text{ °C}$			8	
$\Delta V_{io}/\Delta T$	Input offset voltage drift ⁽¹⁾	$-40\text{ °C} < T < 125\text{ °C}$		10	30	$\text{nV}/\text{°C}$
I_{ib}	Input bias current ($V_{out} = V_{CC}/2$)	$T = 25\text{ °C}$		70	200 ⁽²⁾	pA
		$-40\text{ °C} < T < 125\text{ °C}$			300 ⁽²⁾	
I_{io}	Input offset current ($V_{out} = V_{CC}/2$)	$T = 25\text{ °C}$		140	400 ⁽²⁾	pA
		$-40\text{ °C} < T < 125\text{ °C}$			600 ⁽²⁾	
CMR	Common mode rejection ratio $20 \log (\Delta V_{icm}/\Delta V_{io})$ $V_{ic} = 0\text{ V}$ to $V_{CC}/2$, $V_{out} = V_{CC}/2$ $R_L > 1\text{ M}\Omega$	$T = 25\text{ °C}$	115	136		dB
		$-40\text{ °C} < T < 125\text{ °C}$	115			
SVR	Supply voltage rejection ratio $20 \log (\Delta V_{CC}/\Delta V_{io})$ $V_{CC}/ = 1.8$ to 5.5 V , $V_{out} = V_{CC}/2$, $R_L > 1\text{ M}\Omega$	$T = 25\text{ °C}$	120	140		dB
		$-40\text{ °C} < T < 125\text{ °C}$	120			
A_{vd}	Large signal voltage gain $V_{out} = 0.5\text{ V}$ to $(V_{cc} - 0.5\text{ V})$	$T = 25\text{ °C}$	120	135		dB
		$-40\text{ °C} < T < 125\text{ °C}$	110			
EMIRR ⁽³⁾	EMI rejection ratio EMIRR = $-20 \log (V_{RFpeak}/\Delta V_{io})$	$V_{RF} = 100\text{ mV}_p$, $f = 400\text{ MHz}$		84		dB
		$V_{RF} = 100\text{ mV}_p$, $f = 900\text{ MHz}$		87		
		$V_{RF} = 100\text{ mV}_p$, $f = 1800\text{ MHz}$		90		
		$V_{RF} = 100\text{ mV}_p$, $f = 2400\text{ MHz}$		91		
V_{OH}	High level output voltage	$T = 25\text{ °C}$			30	mV
		$-40\text{ °C} < T < 125\text{ °C}$			70	
V_{OL}	Low level output voltage	$T = 25\text{ °C}$			30	mV
		$-40\text{ °C} < T < 125\text{ °C}$			70	
I_{out}	I_{sink} ($V_{out} = V_{CC}/2$)	$T = 25\text{ °C}$	15	18		mA
		$-40\text{ °C} < T < 125\text{ °C}$	14			
	I_{source} ($V_{out} = 0\text{ V}$)	$T = 25\text{ °C}$	14	17		
		$-40\text{ °C} < T < 125\text{ °C}$	12			
I_{CC}	Supply current (per channel, $V_{out} = V_{CC}/2$, $R_L > 1\text{ M}\Omega$)	$T = 25\text{ °C}$		31	40	μA
		$-40\text{ °C} < T < 125\text{ °C}$			40	

Table 6. Electrical characteristics (continued)

Symbol	Parameter	Conditions	Min.	Typ.	Max.	Unit
AC performance						
GBP	Gain bandwidth product	$R_L = 10\text{ k}\Omega$, $C_L = 100\text{ pF}$		400		kHz
F_u	Unity gain frequency			300		
Φ_m	Phase margin	$R_L = 10\text{ k}\Omega$, $C_L = 100\text{ pF}$		53		degrees
G_m	Gain margin			19		dB
SR	Slew rate ⁽⁴⁾			0.19		V/ μ s
t_s	Settling time	To 0.1%, $V_{in} = 100\text{ mVp-p}$, $R_L = 10\text{ k}\Omega$, $C_L = 100\text{ pF}$		10		μ s
e_n	Equivalent input noise voltage	f = 1 kHz f = 10 kHz		37 37		$\frac{nV}{\sqrt{Hz}}$
C_s	Channel separation	f = 100 Hz		120		dB
t_{init}	Initialization time	T = 25 °C		50		μ s
		-40 °C < T < 125 °C		100		

1. See [Section 4.5: Input offset voltage drift over temperature](#). Input offset measurements are performed on x100 gain configuration. The amplifiers and the gain setting resistors are at the same temperature.
2. Guaranteed by design.
3. Tested on SC-70 package
4. Slew rate value is calculated as the average between positive and negative slew rates.

Figure 2. Supply current vs. supply voltage

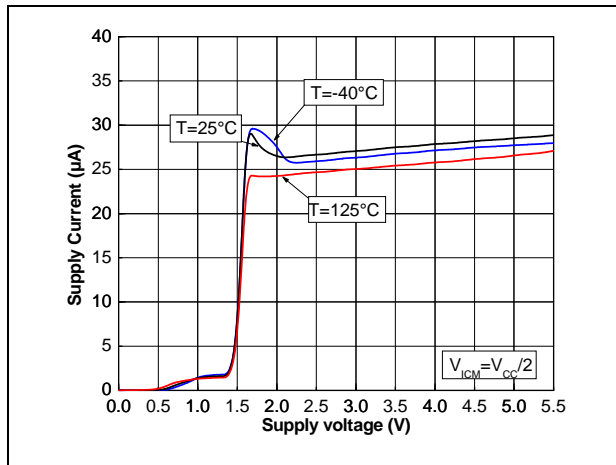


Figure 3. Input offset voltage distribution at $V_{CC} = 5V$

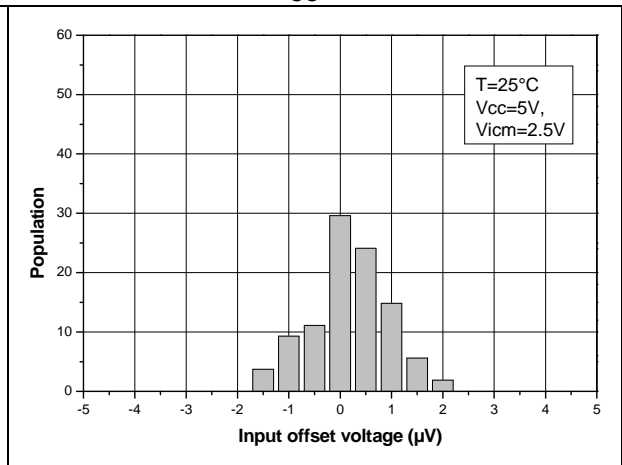


Figure 4. Input offset voltage distribution at $V_{CC} = 3.3V$

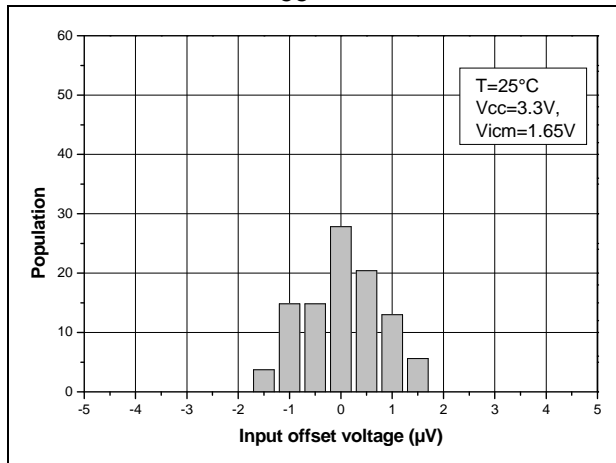


Figure 5. Input offset voltage distribution at $V_{CC} = 1.8V$

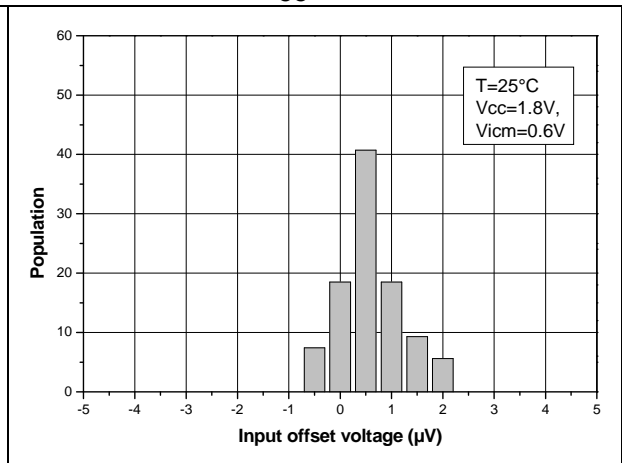


Figure 6. Vio temperature co-efficient distribution (-40 °C to 25 °C)

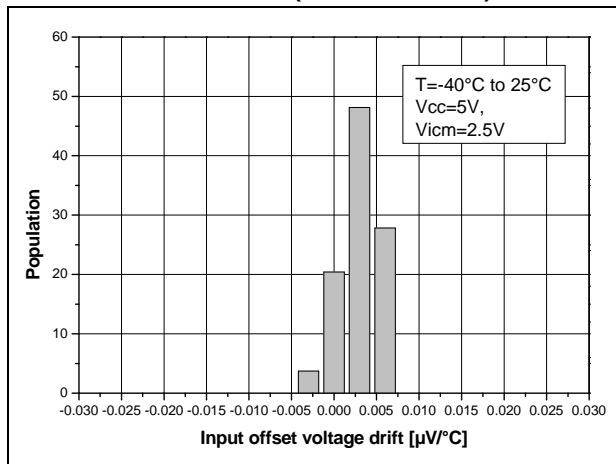


Figure 7. Vio temperature co-efficient distribution (25 °C to 125 °C)

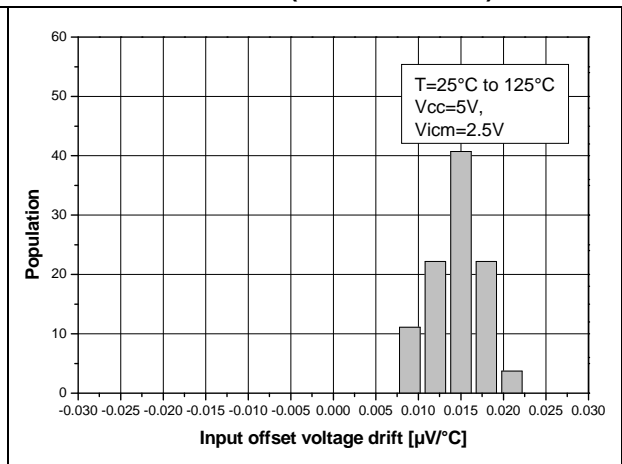


Figure 8. Input offset voltage vs. supply voltage Figure 9. Input offset voltage vs. input common mode at $V_{CC} = 1.8\text{ V}$

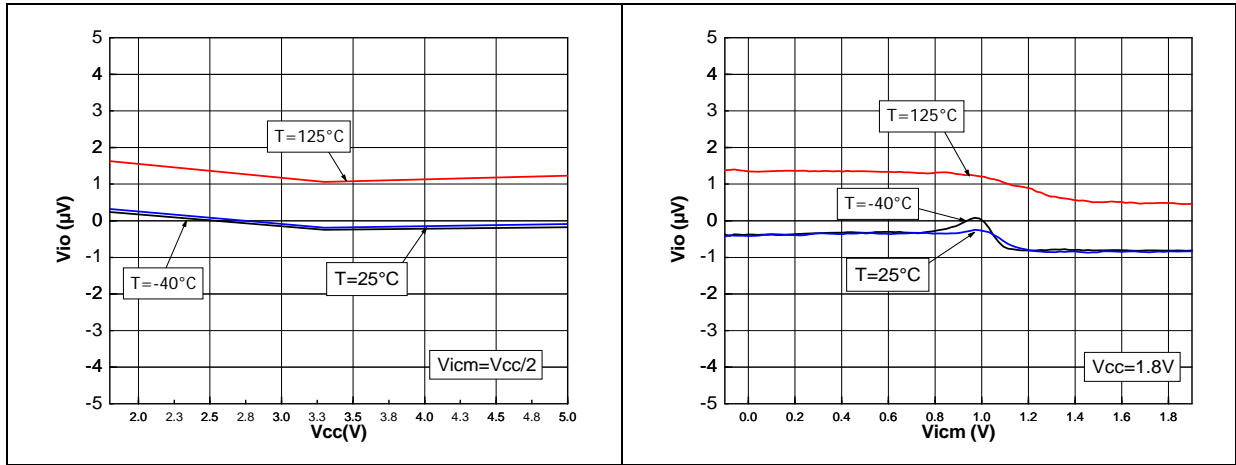


Figure 10. Input offset voltage vs. input common mode at $V_{CC} = 2.7\text{ V}$

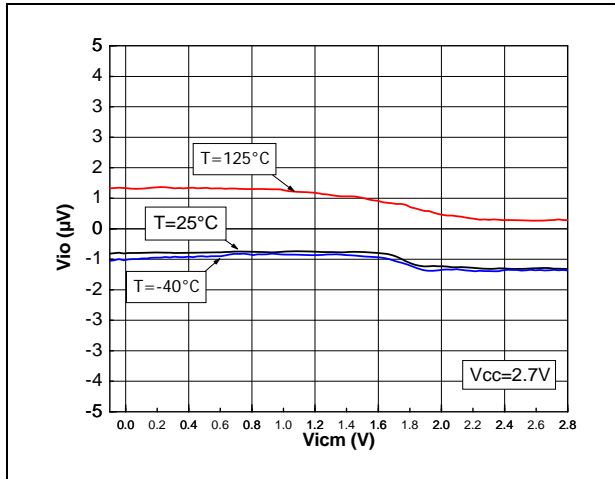


Figure 11. Input offset voltage vs. input common mode at $V_{CC} = 5.5\text{ V}$

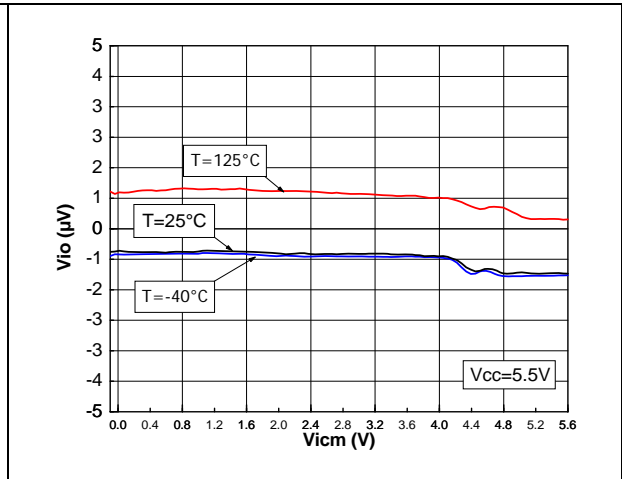


Figure 12. Input offset voltage vs. temperature

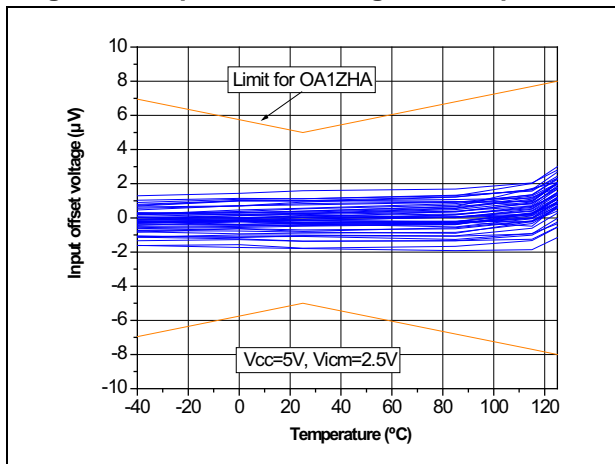


Figure 13. V_{OH} vs. supply voltage

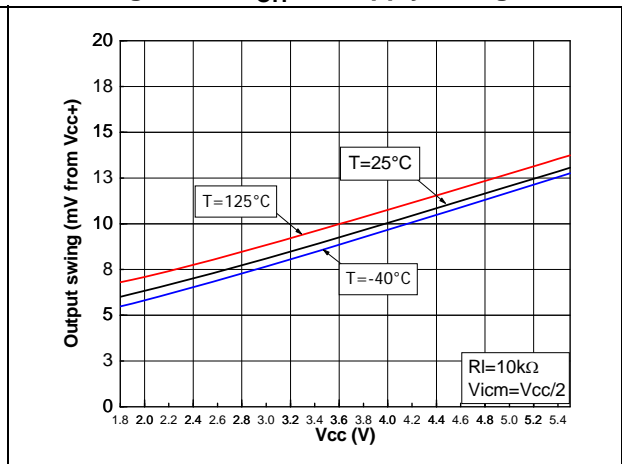


Figure 14. V_{OL} vs. supply voltage

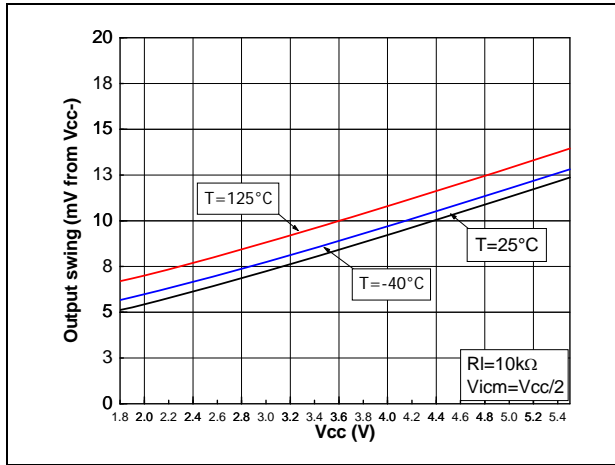


Figure 15. Output current vs. output voltage at $V_{CC} = 1.8\text{ V}$

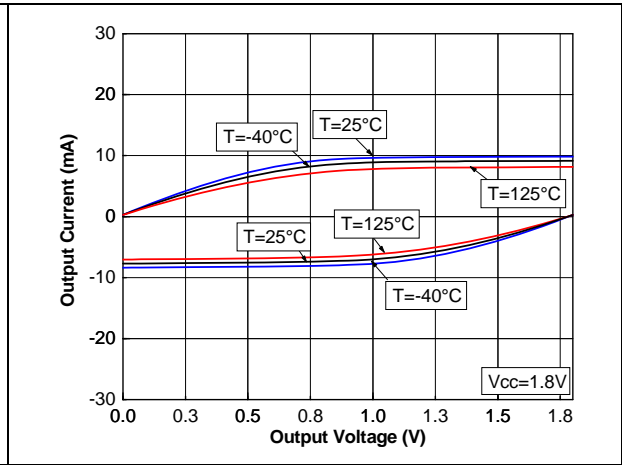


Figure 16. Output current vs. output voltage at $V_{CC} = 5.5\text{ V}$

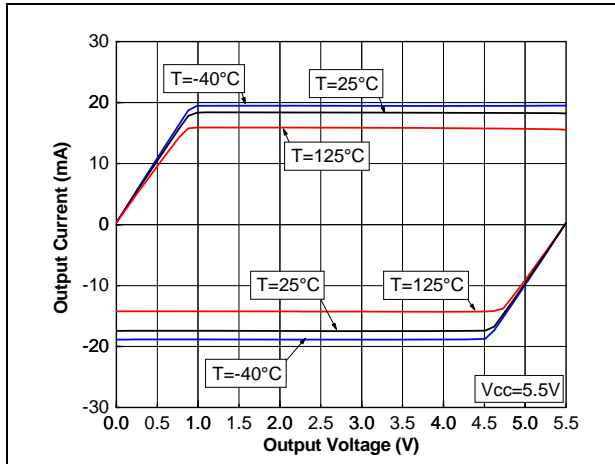


Figure 17. Input bias current vs. common mode at $V_{CC} = 5\text{ V}$

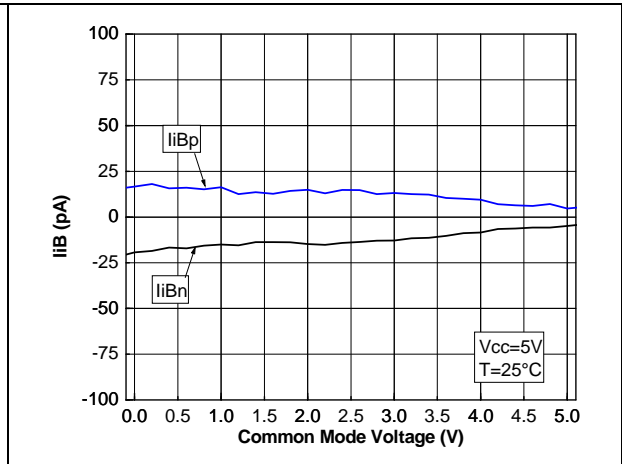


Figure 18. Input bias current vs. common mode at $V_{CC} = 1.8\text{ V}$

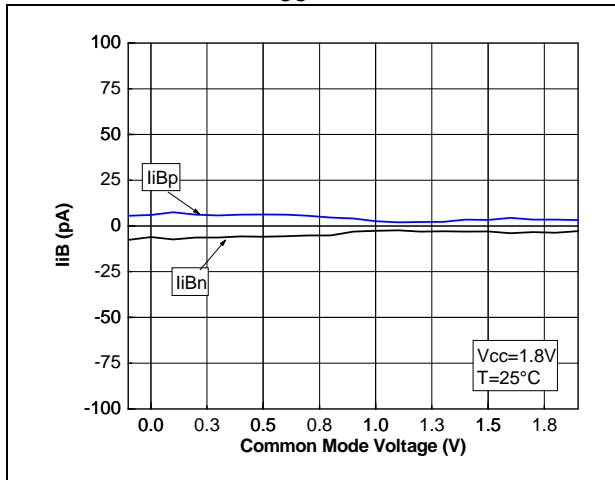


Figure 19. Input bias current vs. temperature at $V_{CC} = 5\text{ V}$

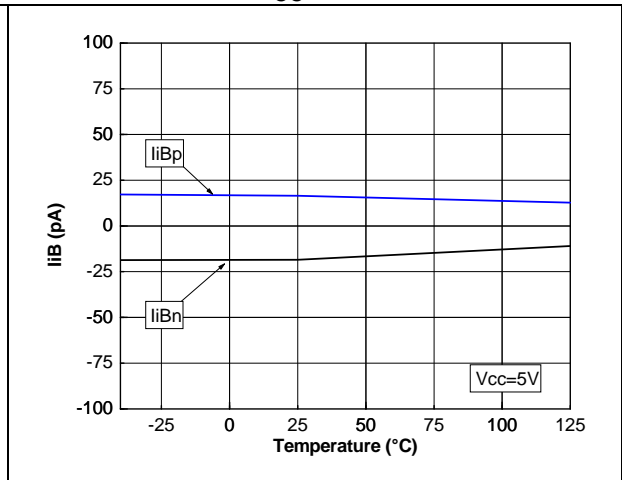


Figure 20. Bode diagram at $V_{CC} = 1.8\text{ V}$

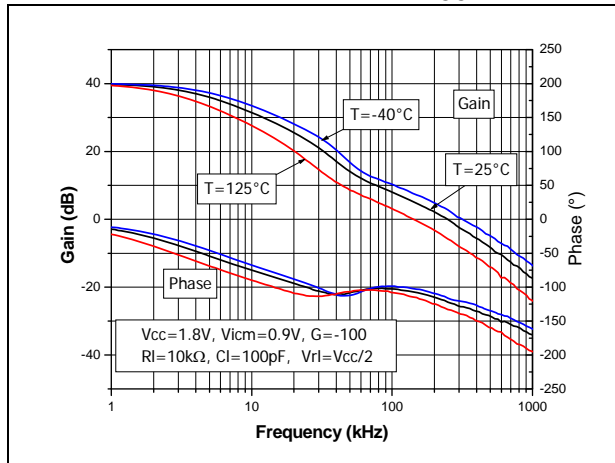


Figure 21. Bode diagram at $V_{CC} = 2.7\text{ V}$

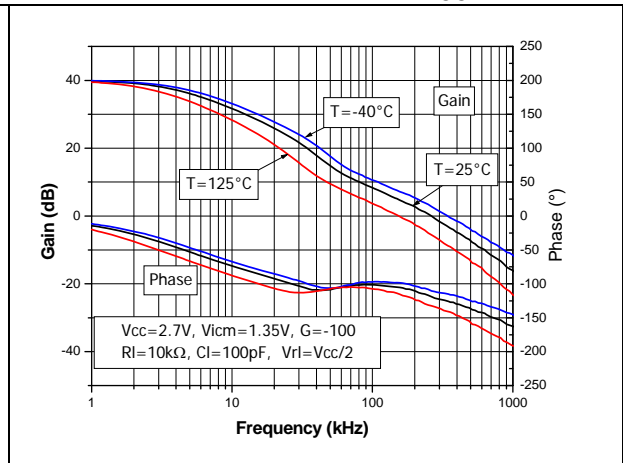


Figure 22. Bode diagram at $V_{CC} = 5.5\text{ V}$

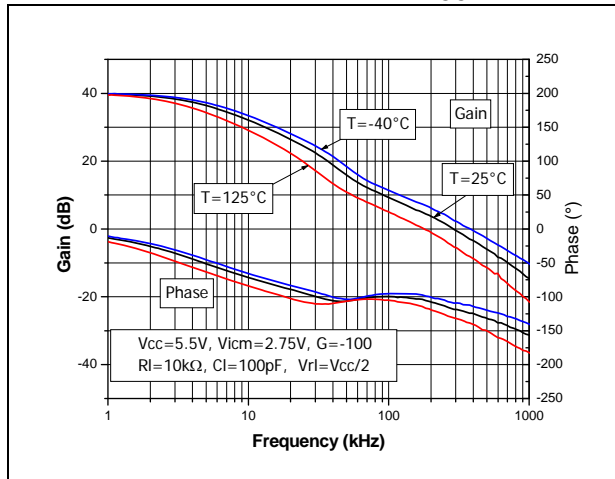


Figure 23. Open loop gain vs. frequency

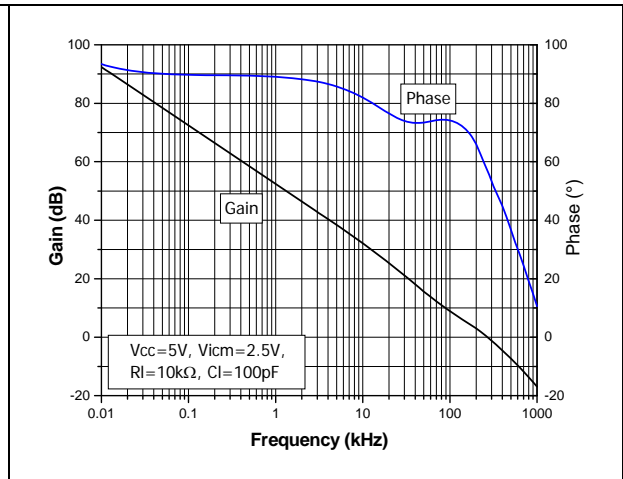


Figure 24. Positive slew rate vs. supply voltage Figure 25. Negative slew rate vs. supply voltage

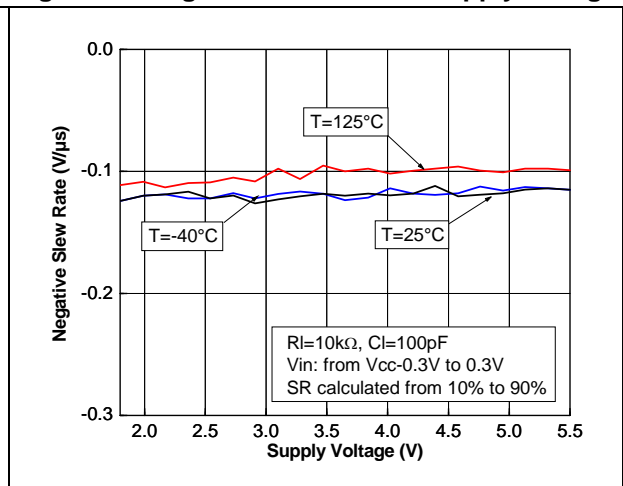
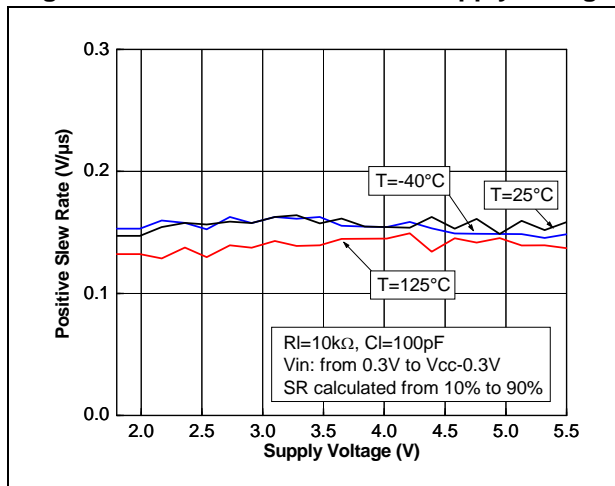


Figure 26. 0.1 Hz to 10 Hz noise

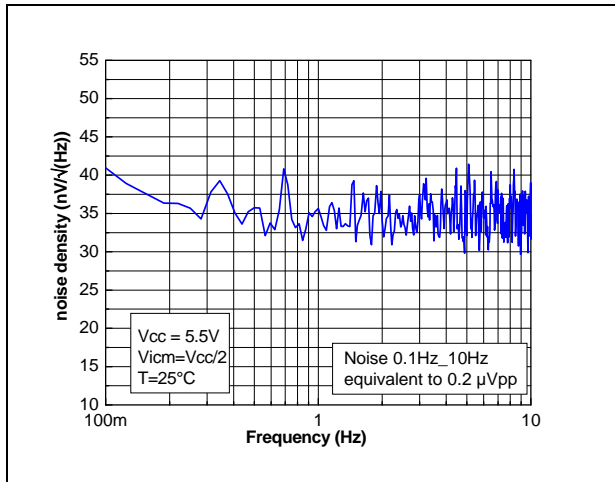


Figure 27. Noise vs. frequency

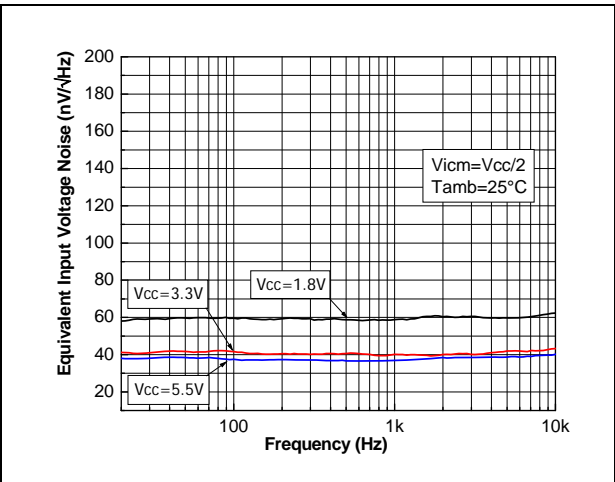


Figure 28. Noise vs. frequency and temperature

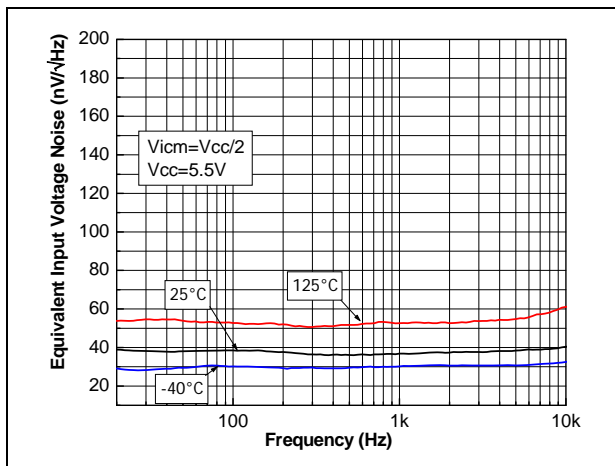


Figure 29. Output overshoot vs. load capacitance

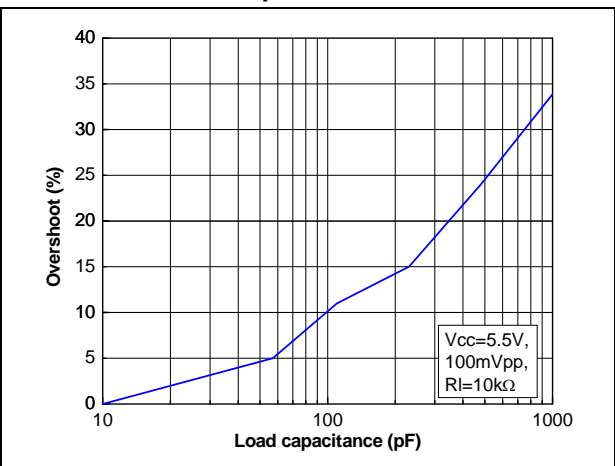


Figure 30. Small signal

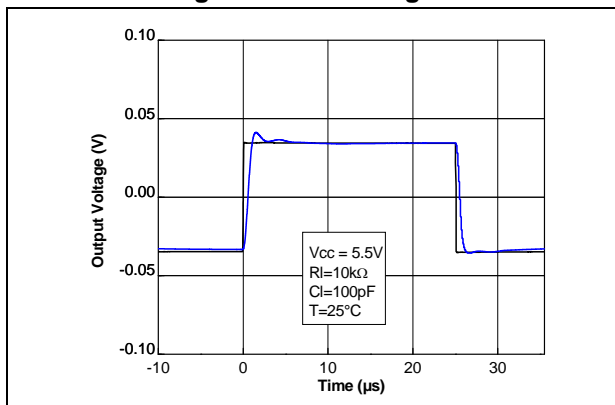


Figure 31. Large signal

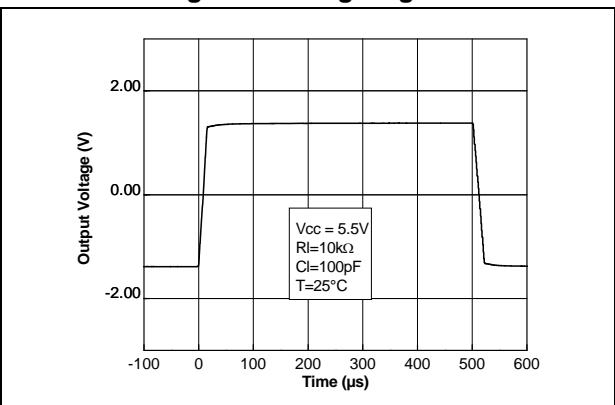


Figure 32. Positive overvoltage recovery at $V_{CC} = 1.8\text{ V}$

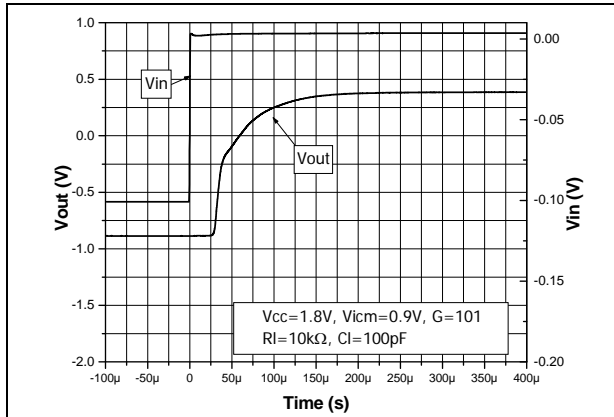


Figure 33. Positive overvoltage recovery at $V_{CC} = 5\text{ V}$

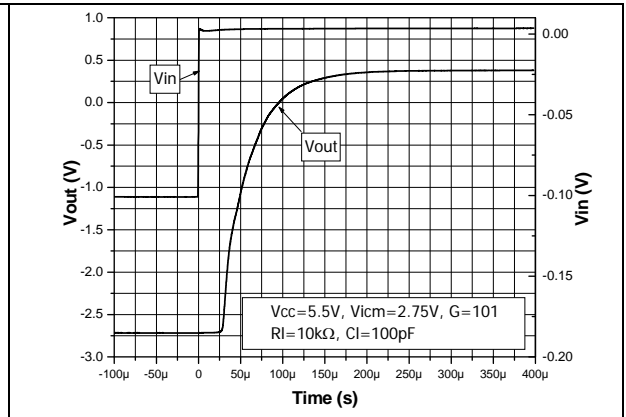


Figure 34. Negative overvoltage recovery at $V_{CC} = 1.8\text{ V}$

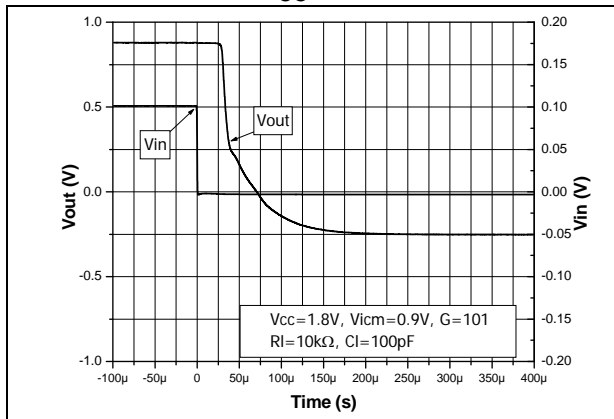


Figure 35. Negative overvoltage recovery at $V_{CC} = 5\text{ V}$

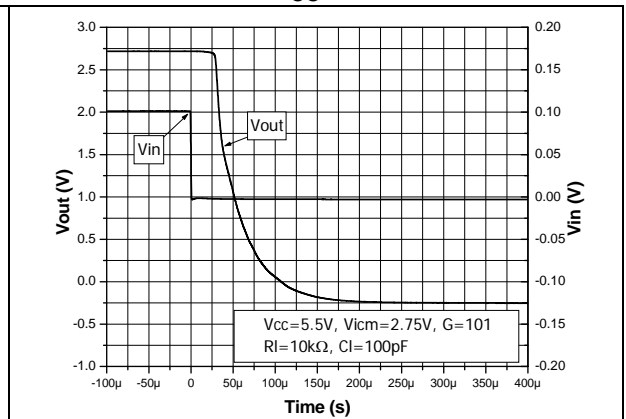


Figure 36. PSRR vs. frequency

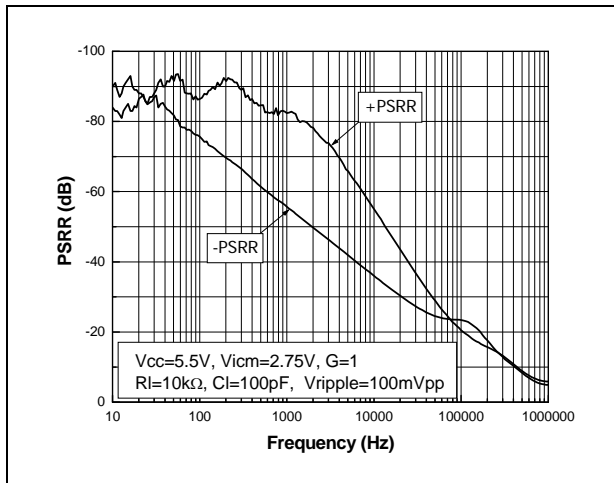
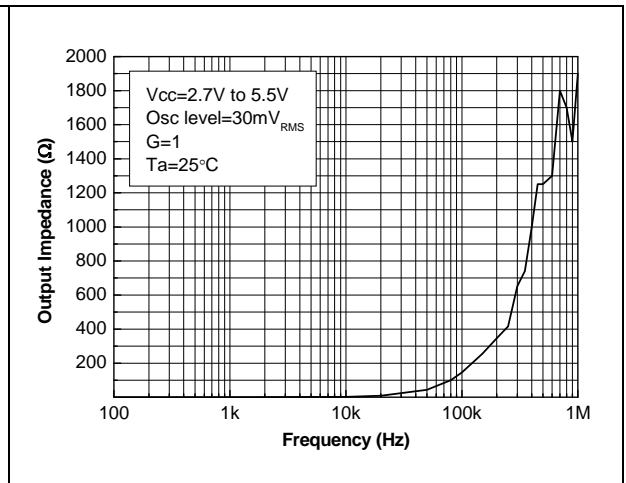


Figure 37. Output impedance vs. frequency



4 Application information

4.1 Operation theory

The OA1ZHA, OA2ZHA and OA4ZHA are high precision CMOS op amp. They achieve a low offset drift and no 1/f noise thanks to their chopper architecture. Chopper-stabilized amps constantly correct low-frequency errors across the inputs of the amplifier.

Chopper-stabilized amplifiers can be explained with respect to:

- Time domain
- Frequency domain

4.1.1 Time domain

The basis of the chopper amplifier is realized in two steps. These steps are synchronized thanks to a clock running at 400 kHz.

Figure 38. Block diagram in the time domain (step 1)

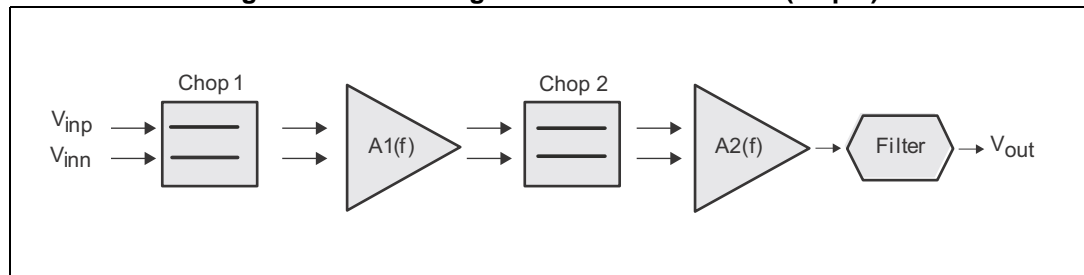


Figure 39. Block diagram in the time domain (step 2)

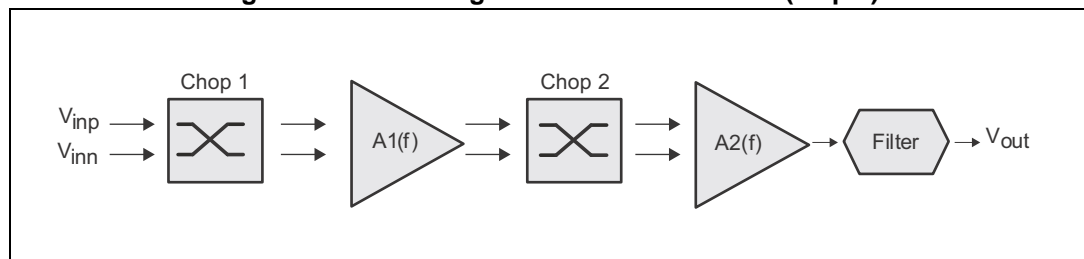


Figure 38 shows step 1, the first clock cycle, where V_{io} is amplified in the normal way.

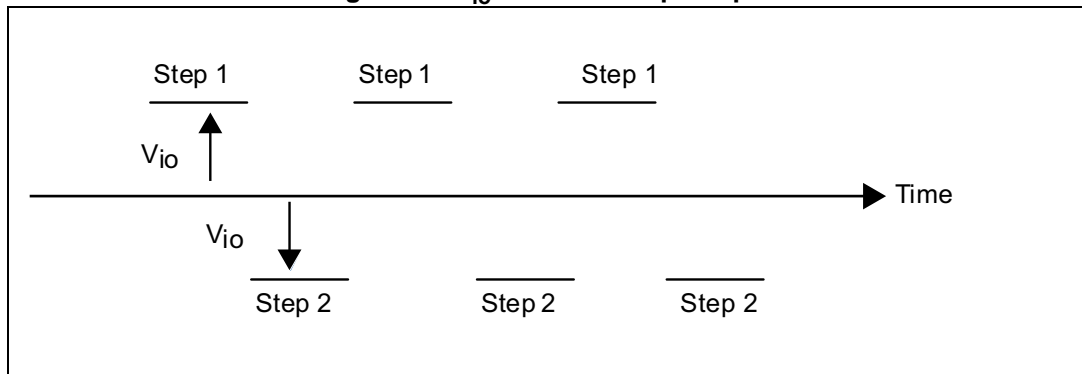
Figure 39 shows step 2, the second clock cycle, where Chop1 and Chop2 swap paths. At this time, the V_{io} is amplified in a reverse way as compared to step 1.

At the end of these two steps, the average V_{io} is close to zero.

The $A2(f)$ amplifier has a small impact on the V_{io} because the V_{io} is expressed as the input offset and is consequently divided by $A1(f)$.

In the time domain, the offset part of the output signal before filtering is shown in [Figure 40](#).

Figure 40. V_{io} cancellation principle



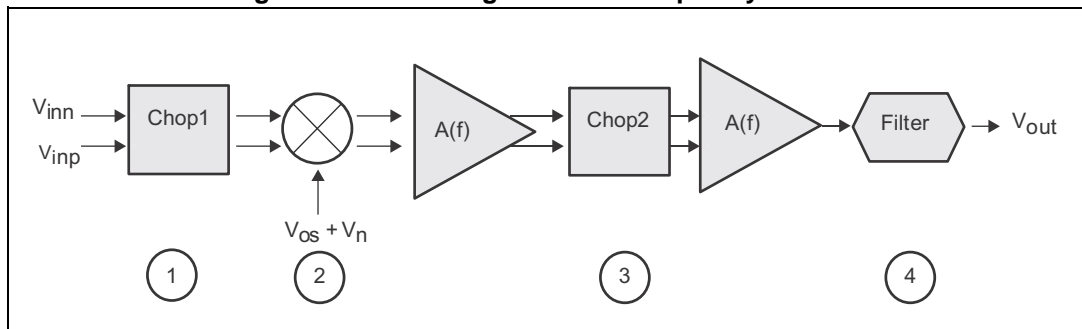
The low pass filter averages the output value resulting in the cancellation of the V_{io} offset.

The $1/f$ noise can be considered as an offset in low frequency and it is canceled like the V_{io} , thanks to the chopper technique.

4.1.2 Frequency domain

The frequency domain gives a more accurate vision of chopper-stabilized amplifier architecture.

Figure 41. Block diagram in the frequency domain



The modulation technique transposes the signal to a higher frequency where there is no $1/f$ noise, and demodulate it back after amplification.

1. According to [Figure 41](#), the input signal V_{in} is modulated once (Chop1) so all the input signal is transposed to the high frequency domain.
2. The amplifier adds its own error (V_{io} (output offset voltage) + the noise V_n ($1/f$ noise)) to this modulated signal.
3. This signal is then demodulated (Chop2), but since the noise and the offset are modulated only once, they are transposed to the high frequency, leaving the output signal of the amplifier without any offset and low frequency noise. Consequently, the input signal is amplified with a very low offset and $1/f$ noise.
4. To get rid of the high frequency part of the output signal (which is useless) a low pass filter is implemented.

To further suppress the remaining ripple down to a desired level, another low pass filter may be added externally on the output of the OA1ZHA, OA2ZHA and OA4ZHA device.

4.2 Operating voltages

OA1ZHA, OA2ZHA and OA4ZHA CMOS op amp can operate from 1.8 to 5.5 V. The parameters are fully specified for 1.8 V, 3.3 V, and 5 V power supplies. However, the parameters are very stable in the full V_{CC} range and several characterization curves show the OA1ZHA, OA2ZHA and OA4ZHA op amp characteristics at 1.8 V and 5.5 V. Additionally, the main specifications are guaranteed in extended temperature ranges from -40 to +125 °C.

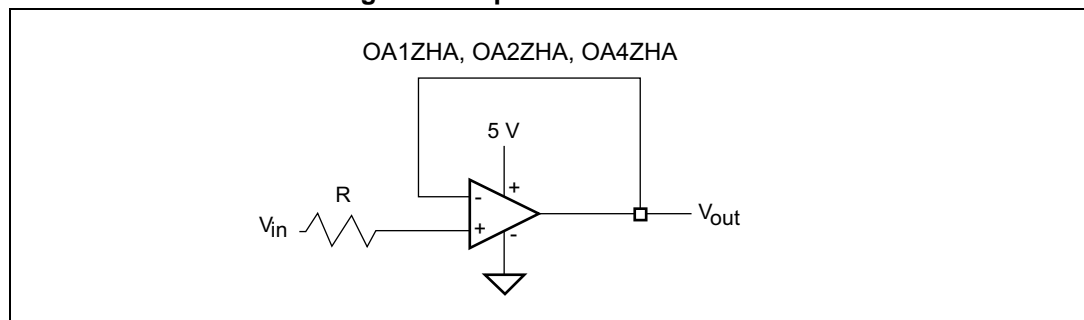
4.3 Input pin voltage ranges

OA1ZHA, OA2ZHA and OA4ZHA CMOS op amp can operate from 1.8 to 5.5 V. The parameters are fully specified for 1.8 V, 3.3 V, and have internal ESD diode protection on the inputs. These diodes are connected between the input and each supply rail to protect the input MOSFETs from electrical discharge.

If the input pin voltage exceeds the power supply by 0.5 V, the ESD diodes become conductive and excessive current can flow through them. Without limitation this over current can damage the device.

In this case, it is important to limit the current to 10 mA, by adding resistance on the input pin, as described in [Figure 42](#).

Figure 42. Input current limitation



4.4 Rail-to-rail input

OA1ZHA, OA2ZHA and OA4ZHA CMOS op amp have a rail-to-rail input, and the input common mode range is extended from $V_{CC-} - 0.1$ V to $V_{CC+} + 0.1$ V.

4.5 Input offset voltage drift over temperature

The maximum input voltage drift variation over temperature is defined as the offset variation related to the offset value measured at 25 °C. The operational amplifier is one of the main circuits of the signal conditioning chain, and the amplifier input offset is a major contributor to the chain accuracy. The signal chain accuracy at 25 °C can be compensated during production at application level. The maximum input voltage drift over temperature enables the system designer to anticipate the effect of temperature variations.

The maximum input voltage drift over temperature is computed using [Equation 1](#).

Equation 1

$$\frac{\Delta V_{io}}{\Delta T} = \max \left| \frac{V_{io}(T) - V_{io}(25^{\circ}\text{C})}{T - 25^{\circ}\text{C}} \right|$$

where T = -40 °C and 125 °C.

The OA1ZHA, OA2ZHA and OA4ZHA CMOS datasheet maximum value is guaranteed by measurements on a representative sample size ensuring a C_{pk} (process capability index) greater than 1.3.

4.6 Rail-to-rail output

The operational amplifier output levels can go close to the rails: to a maximum of 30 mV above and below the rail when connected to a 10 kΩ resistive load to $V_{CC}/2$.

4.7 Capacitive load

Driving large capacitive loads can cause stability problems. Increasing the load capacitance produces gain peaking in the frequency response, with overshoot and ringing in the step response. It is usually considered that with a gain peaking higher than 2.3 dB an op amp might become unstable.

Generally, the unity gain configuration is the worst case for stability and the ability to drive large capacitive loads.

[Figure 43](#) and [Figure 44](#) show the serial resistor that must be added to the output, to make a system stable. [Figure 45](#) shows the test configuration using an isolation resistor, R_{iso} .

Figure 43. Stability criteria with a serial resistor at $V_{DD} = 5\text{ V}$ **Figure 44. Stability criteria with a serial resistor at $V_{DD} = 1.8\text{ V}$**

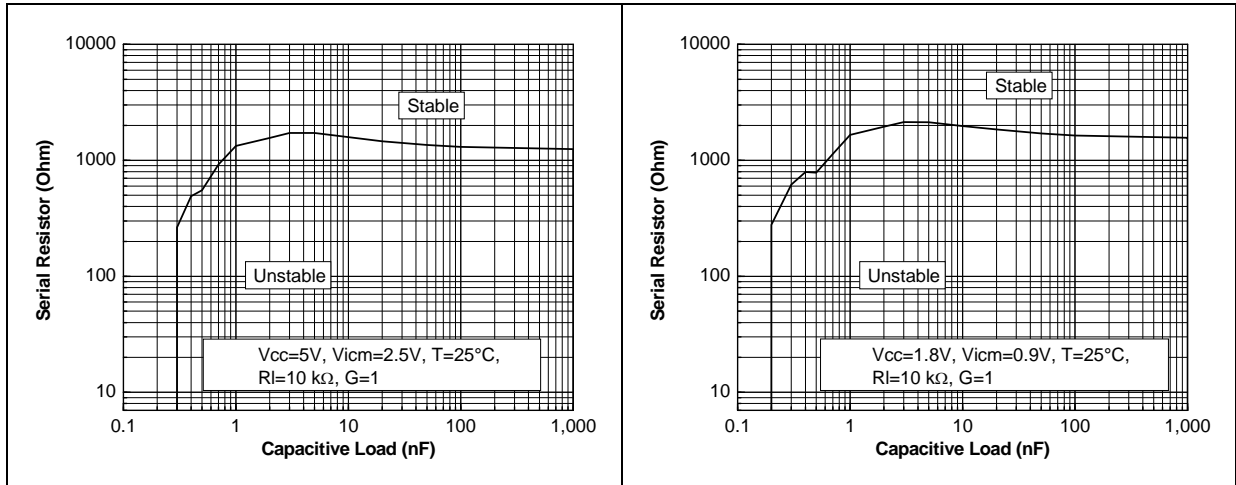
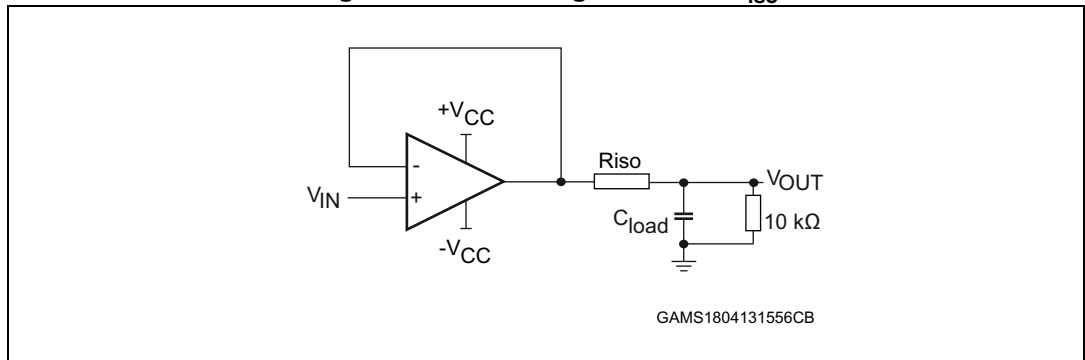


Figure 45. Test configuration for R_{iso}



4.8 PCB layout recommendations

Particular attention must be paid to the layout of the PCB, tracks connected to the amplifier, load, and power supply. The power and ground traces are critical as they must provide adequate energy and grounding for all circuits. Good practice is to use short and wide PCB traces to minimize voltage drops and parasitic inductance.

In addition, to minimize parasitic impedance over the entire surface, a multi-via technique that connects the bottom and top layer ground planes together in many locations is often used.

The copper traces that connect the output pins to the load and supply pins should be as wide as possible to minimize trace resistance.

4.9 Optimized application recommendation

OA1ZHA, OA2ZHA and OA4ZHA CMOS op amp are based on chopper architecture. As they are switched devices, it is strongly recommended to place a 0.1 μF capacitor as close as possible to the supply pins.

A good decoupling has several advantages for an application. First, it helps to reduce electromagnetic interference. Due to the modulation of the chopper, the decoupling capacitance also helps to reject the small ripple that may appear on the output.

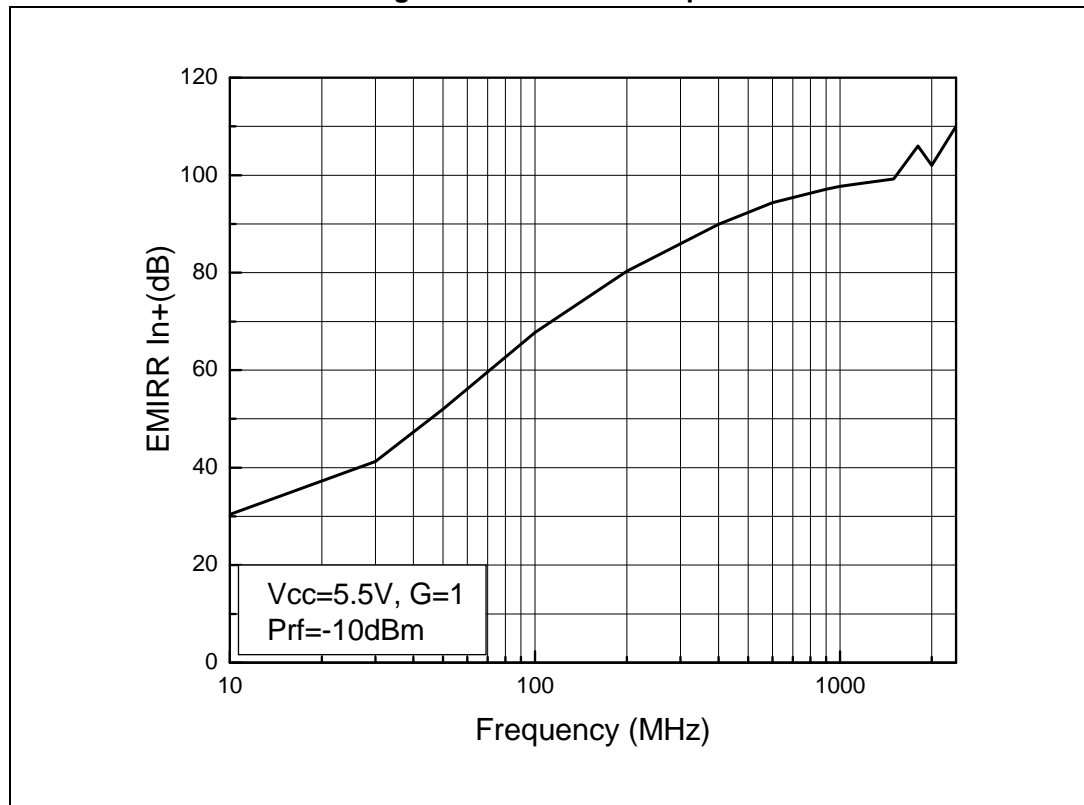
OA1ZHA, OA2ZHA and OA4ZHA CMOS op amp have been optimized for use with 10 k Ω in the feedback loop. With this, or a higher value of resistance, these devices offer the best performance.

4.10 EMI rejection ration (EMIRR)

The electromagnetic interference (EMI) rejection ratio, or EMIRR, describes the EMI immunity of operational amplifiers. An adverse effect that is common to many op amp is a change in the offset voltage as a result of RF signal rectification.

OA1ZHA, OA2ZHA and OA4ZHA CMOS op amp have been specially designed to minimize susceptibility to EMIRR and show an extremely good sensitivity. *Figure 46* shows the EMIRR IN+ of the OA1ZHA, OA2ZHA and OA4ZHA measured from 10 MHz up to 2.4 GHz.

Figure 46. EMIRR on IN+ pin

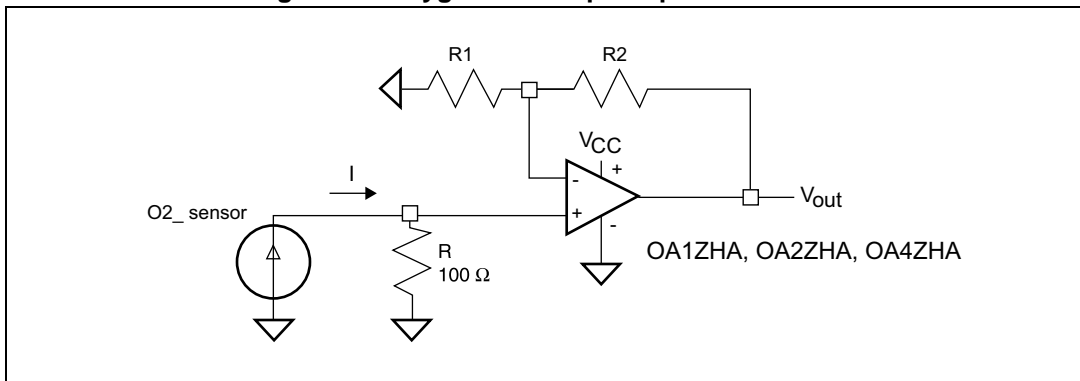


4.11 Application examples

4.11.1 Oxygen sensor

The electrochemical sensor creates a current proportional to the concentration of the gas being measured. This current is converted into voltage thanks to R resistance. This voltage is then amplified by OA1ZHA, OA2ZHA and OA4ZHA CMOS op amp (see [Figure 47](#)).

Figure 47. Oxygen sensor principle schematic



The output voltage is calculated using [Equation 2](#):

Equation 2

$$V_{out} = (I \times R - V_{io}) \times \left(\frac{R_2}{R_1} + 1 \right)$$

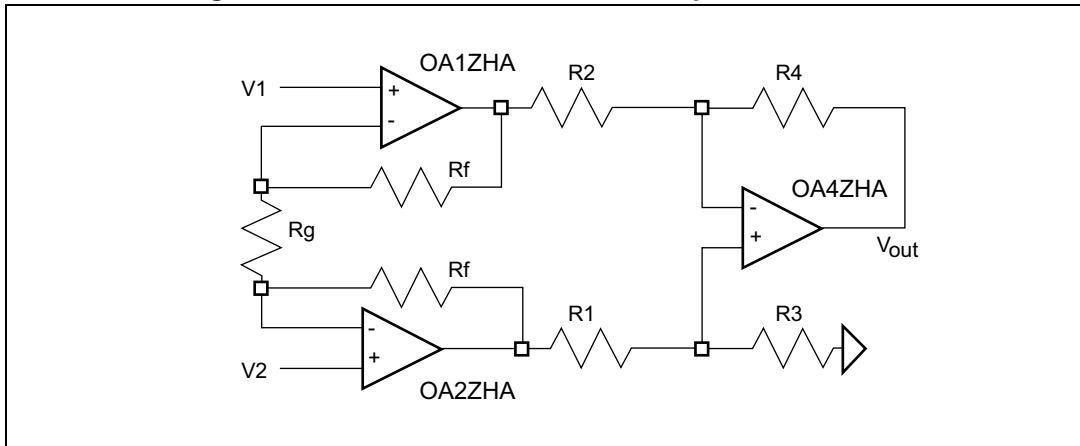
As the current delivered by the O2 sensor is extremely low, the impact of the V_{io} can become significant with a traditional operational amplifier. The use of the chopper amplifier of the OA1ZHA, OA2ZHA and OA4ZHA is perfect for this application.

In addition, using OA1ZHA, OA2ZHA and OA4ZHA op amp for the O2 sensor application ensures that the measurement of O2 concentration is stable even at different temperature thanks to a very good $\Delta V_{io}/\Delta T$.

4.11.2 Precision instrumentation amplifier

The instrumentation amplifier uses three op amp. The circuit, shown in [Figure 48](#), exhibits high input impedance, so that the source impedance of the connected sensor has no impact on the amplification.

Figure 48. Precision instrumentation amplifier schematic



The gain is set by tuning the R_g resistor. With $R_1 = R_2$ and $R_3 = R_4$, the output is given by [Equation 3](#).

Equation 3

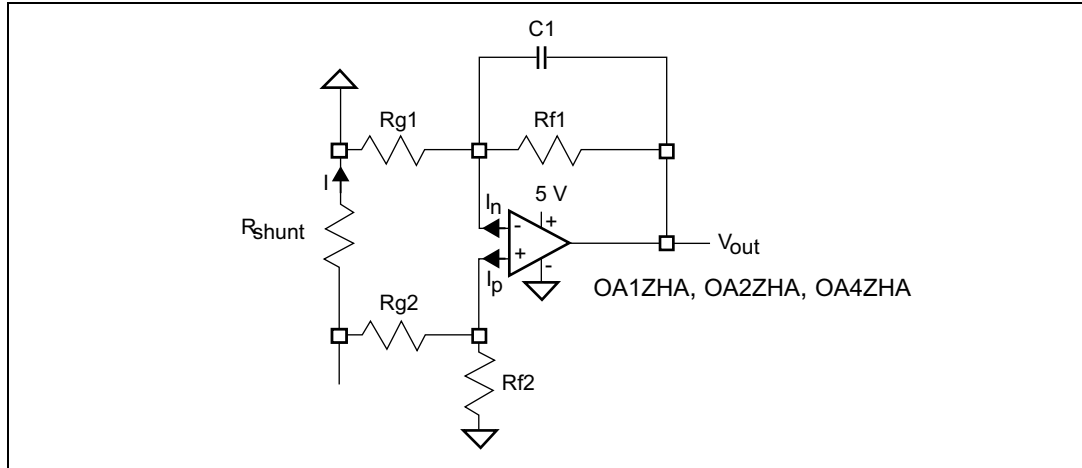
$$V_{out} = (V_2 - V_1) \cdot \left[\frac{R_4}{R_2} \cdot \left(\frac{2R_f}{R_g} + 1 \right) \right]$$

The matching of R_1 , R_2 and R_3 , R_4 is important to ensure a good common mode rejection ratio (CMR).

4.11.3 Low-side current sensing

Power management mechanisms are found in most electronic systems. Current sensing is useful for protecting applications. The low-side current sensing method consists of placing a sense resistor between the load and the circuit ground. The resulting voltage drop is amplified using OA1ZHA, OA2ZHA and OA4ZHA CMOS op amp (see [Figure 49](#)).

Figure 49. Low-side current sensing schematic



V_{out} can be expressed as follows:

Equation 4

$$V_{out} = R_{shunt} \times I \left(1 - \frac{R_{g2}}{R_{g2} + R_{f2}} \right) \left(1 + \frac{R_{f1}}{R_{g1}} \right) + I_p \left(\frac{R_{g2} \times R_{f2}}{R_{g2} + R_{f2}} \right) \times \left(1 + \frac{R_{f1}}{R_{g1}} \right) - I_n \times R_{f1} - V_{io} \left(1 + \frac{R_{f1}}{R_{g1}} \right)$$

Assuming that $R_{f2} = R_{f1} = R_f$ and $R_{g2} = R_{g1} = R_g$, [Equation 4](#) can be simplified as follows:

Equation 5

$$V_{out} = R_{shunt} \times I \left(\frac{R_f}{R_g} \right) - V_{io} \left(1 + \frac{R_f}{R_g} \right) + R_f \times I_{io}$$

The main advantage of using the chopper of the OA1ZHA, OA2ZHA and OA4ZHA, for a low-side current sensing, is that the errors due to V_{io} and I_{io} are extremely low and may be neglected.

Therefore, for the same accuracy, the shunt resistor can be chosen with a lower value, resulting in lower power dissipation, lower drop in the ground path, and lower cost.

Particular attention must be paid on the matching and precision of R_{g1} , R_{g2} , R_{f1} , and R_{f2} , to maximize the accuracy of the measurement.

5 Package information

In order to meet environmental requirements, ST offers these devices in different grades of ECOPACK[®] packages, depending on their level of environmental compliance. ECOPACK[®] specifications, grade definitions and product status are available at: www.st.com. ECOPACK[®] is an ST trademark.

5.1 SC70-5 package information

Figure 50. SC70-5 package mechanical drawing

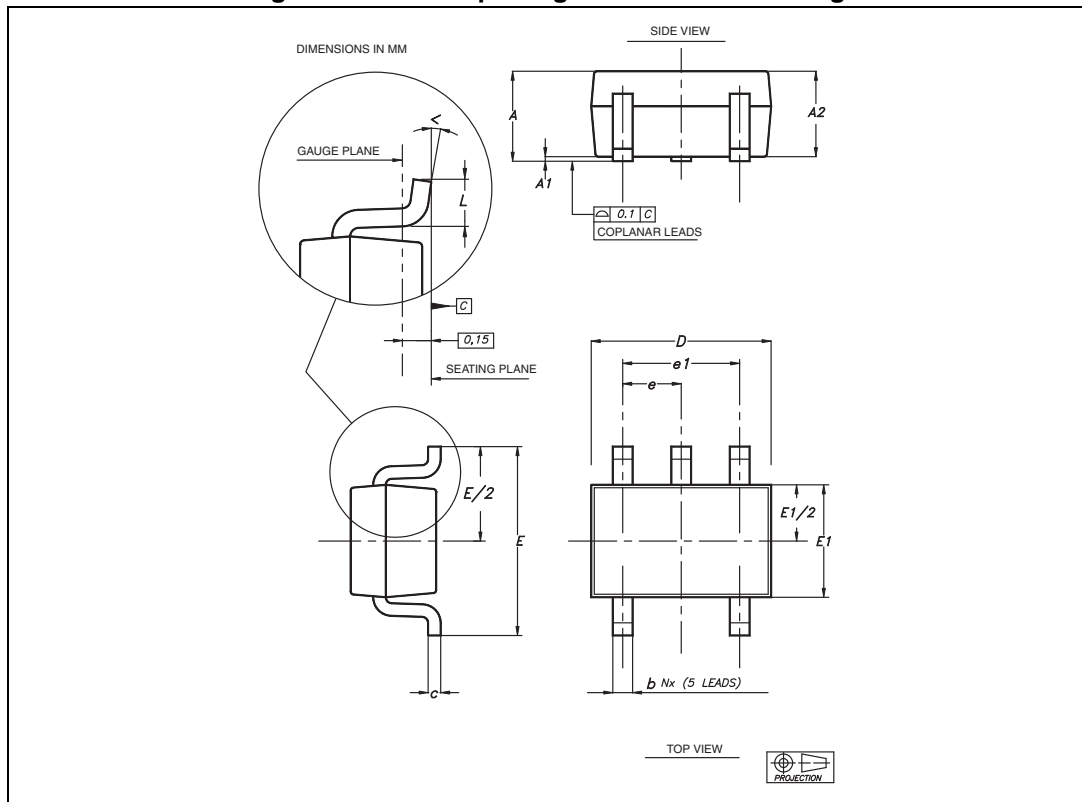


Table 7. SC70-5 package mechanical data

Symbol	Dimensions					
	Millimeters			Inches		
	Min.	Typ.	Max.	Min.	Typ.	Max.
A	0.80		1.10	0.032		0.043
A1	0		0.10			0.004
A2	0.80	0.90	1.00	0.032	0.035	0.039
b	0.15		0.30	0.006		0.012
c	0.10		0.22	0.004		0.009
D	1.80	2.00	2.20	0.071	0.079	0.087
E	1.80	2.10	2.40	0.071	0.083	0.094
E1	1.15	1.25	1.35	0.045	0.049	0.053
e		0.65			0.025	
e1		1.30			0.051	
L	0.26	0.36	0.46	0.010	0.014	0.018
<	0°		8°	0°		8°

5.2 DFN8 2x2 package information

Figure 51. DFN8 2x2 package mechanical drawing

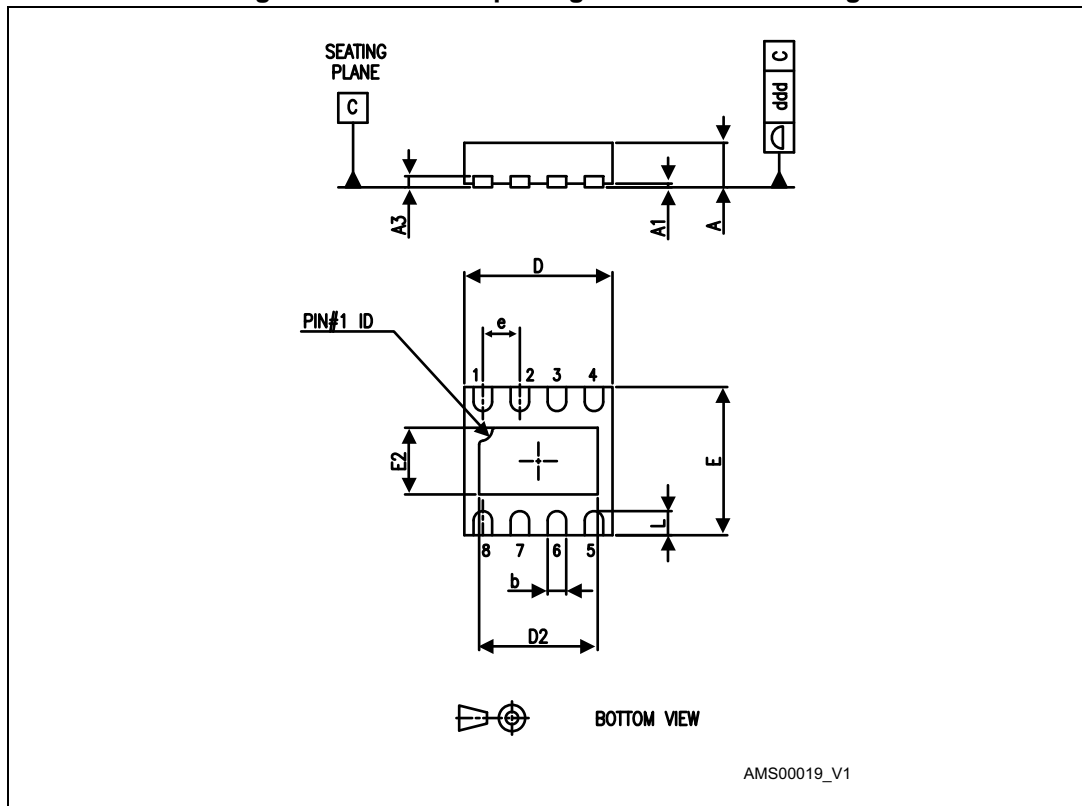
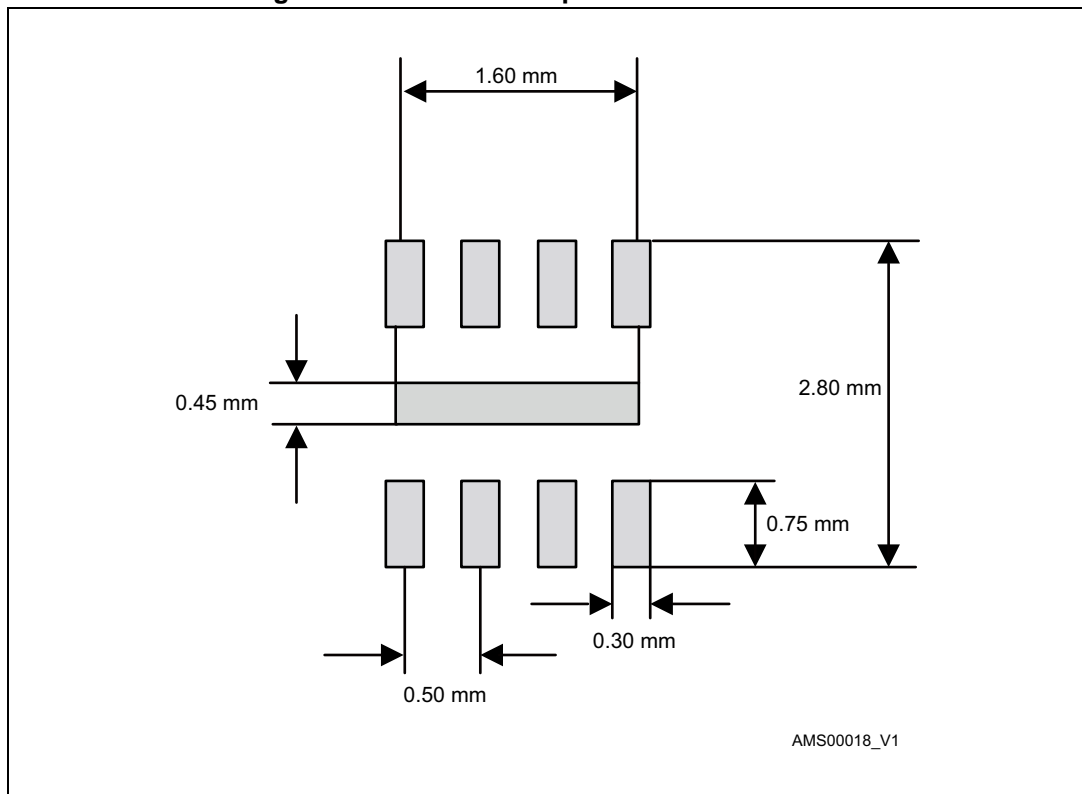


Table 8. DFN8 2x2x0.6 mm package mechanical data (pitch 0.5 mm)

Symbol	Dimensions					
	Millimeters			Inches		
	Min.	Typ.	Max.	Min.	Typ.	Max.
A	0.51	0.55	0.60	0.020	0.022	0.024
A1			0.05			0.002
A3		0.15			0.006	
b	0.18	0.25	0.30	0.007	0.010	0.012
D	1.85	2.00	2.15	0.073	0.079	0.085
D2	1.45	1.60	1.70	0.057	0.063	0.067
E	1.85	2.00	2.15	0.073	0.079	0.085
E2	0.75	0.90	1.00	0.030	0.035	0.039
e		0.50			0.020	
L			0.425			0.017
ddd			0.08			0.003

Figure 52. DFN8 2x2 footprint recommendation



5.3 MiniSO8 package information

Figure 53. MiniSO8 package mechanical drawing

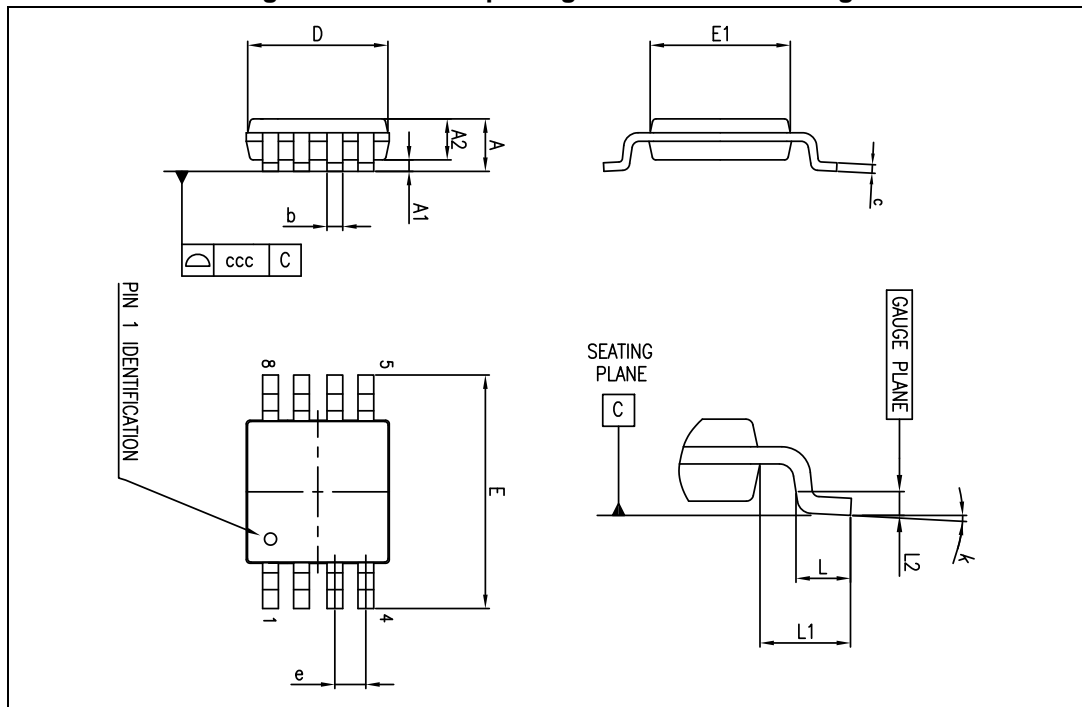


Table 9. MiniSO8 package mechanical data

Symbol	Dimensions					
	Millimeters			Inches		
	Min.	Typ.	Max.	Min.	Typ.	Max.
A			1.1			0.043
A1	0		0.15	0		0.006
A2	0.75	0.85	0.95	0.030	0.033	0.037
b	0.22		0.40	0.009		0.016
c	0.08		0.23	0.003		0.009
D	2.80	3.00	3.20	0.11	0.118	0.126
E	4.65	4.90	5.15	0.183	0.193	0.203
E1	2.80	3.00	3.10	0.11	0.118	0.122
e		0.65			0.026	
L	0.40	0.60	0.80	0.016	0.024	0.031
L1		0.95			0.037	
L2		0.25			0.010	
k	0°		8°	0°		8°
ccc			0.10			0.004

5.4 QFN16 3x3 package information

Figure 54. QFN16 3x3 package mechanical drawing

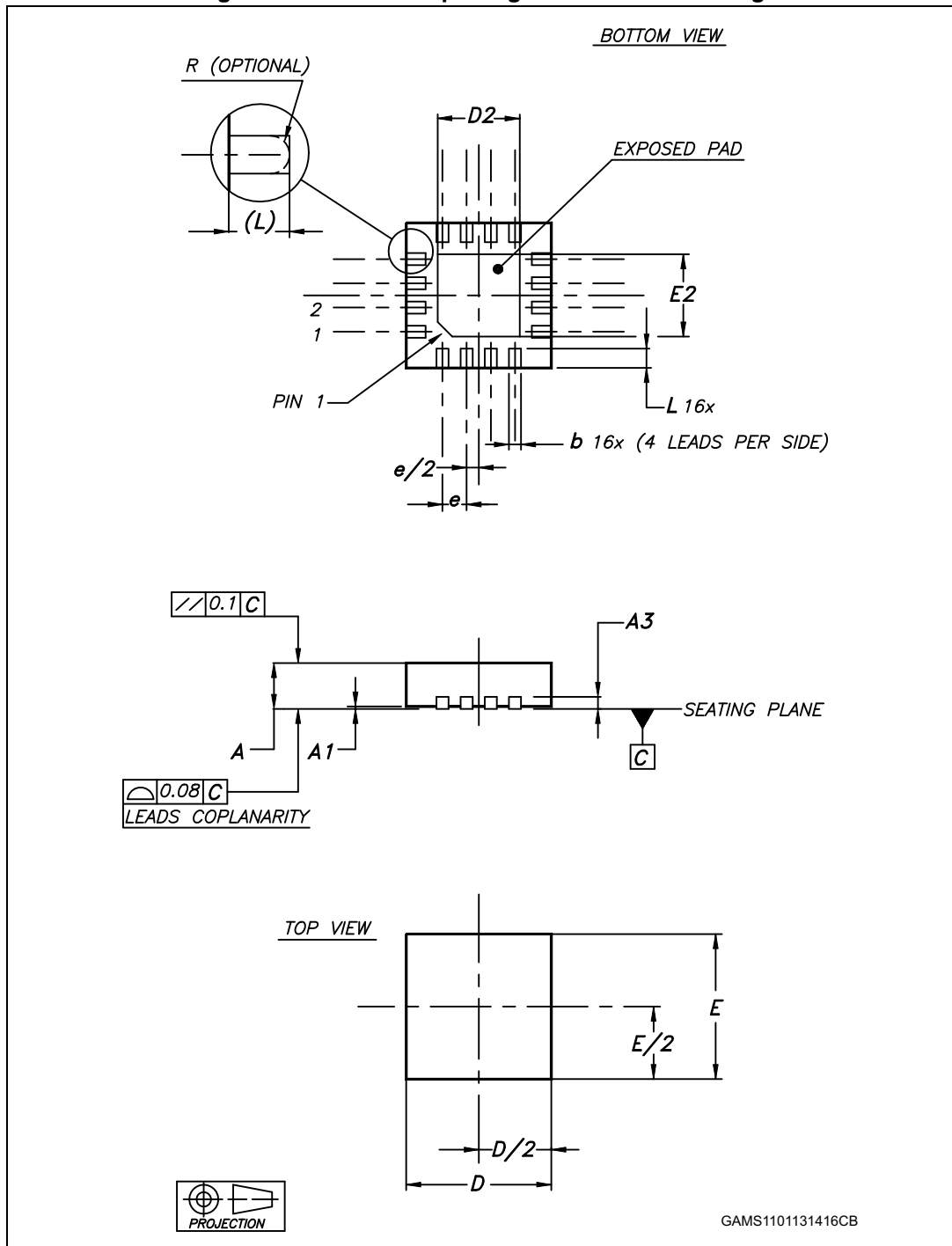


Table 10. QFN16 3 x 3 mm package mechanical data (pitch 0.5 mm)

Symbol	Dimensions					
	Millimeters			Inches		
	Min.	Typ.	Max.	Min.	Typ.	Max.
A	0.80	0.90	1.00	0.031	0.035	0.039
A1	0		0.05	0		0.002
A3		0.20			0.008	
b	0.18		0.30	0.007		0.012
D	2.90	3.00	3.10	0.114	0.118	0.122
D2	1.50		1.80	0.059		0.071
E	2.90	3.00	3.10	0.114	0.118	0.122
E2	1.50		1.80	0.059		0.071
e		0.50			0.020	
L	0.30		0.50	0.012		0.020

6 Revision history

Table 11. Document revision history

Date	Revision	Changes
04-Mar-2014	1	Initial release.

Please Read Carefully:

Information in this document is provided solely in connection with ST products. STMicroelectronics NV and its subsidiaries ("ST") reserve the right to make changes, corrections, modifications or improvements, to this document, and the products and services described herein at any time, without notice.

All ST products are sold pursuant to ST's terms and conditions of sale.

Purchasers are solely responsible for the choice, selection and use of the ST products and services described herein, and ST assumes no liability whatsoever relating to the choice, selection or use of the ST products and services described herein.

No license, express or implied, by estoppel or otherwise, to any intellectual property rights is granted under this document. If any part of this document refers to any third party products or services it shall not be deemed a license grant by ST for the use of such third party products or services, or any intellectual property contained therein or considered as a warranty covering the use in any manner whatsoever of such third party products or services or any intellectual property contained therein.

UNLESS OTHERWISE SET FORTH IN ST'S TERMS AND CONDITIONS OF SALE ST DISCLAIMS ANY EXPRESS OR IMPLIED WARRANTY WITH RESPECT TO THE USE AND/OR SALE OF ST PRODUCTS INCLUDING WITHOUT LIMITATION IMPLIED WARRANTIES OF MERCHANTABILITY, FITNESS FOR A PARTICULAR PURPOSE (AND THEIR EQUIVALENTS UNDER THE LAWS OF ANY JURISDICTION), OR INFRINGEMENT OF ANY PATENT, COPYRIGHT OR OTHER INTELLECTUAL PROPERTY RIGHT.

ST PRODUCTS ARE NOT DESIGNED OR AUTHORIZED FOR USE IN: (A) SAFETY CRITICAL APPLICATIONS SUCH AS LIFE SUPPORTING, ACTIVE IMPLANTED DEVICES OR SYSTEMS WITH PRODUCT FUNCTIONAL SAFETY REQUIREMENTS; (B) AERONAUTIC APPLICATIONS; (C) AUTOMOTIVE APPLICATIONS OR ENVIRONMENTS, AND/OR (D) AEROSPACE APPLICATIONS OR ENVIRONMENTS. WHERE ST PRODUCTS ARE NOT DESIGNED FOR SUCH USE, THE PURCHASER SHALL USE PRODUCTS AT PURCHASER'S SOLE RISK, EVEN IF ST HAS BEEN INFORMED IN WRITING OF SUCH USAGE, UNLESS A PRODUCT IS EXPRESSLY DESIGNATED BY ST AS BEING INTENDED FOR "AUTOMOTIVE, AUTOMOTIVE SAFETY OR MEDICAL" INDUSTRY DOMAINS ACCORDING TO ST PRODUCT DESIGN SPECIFICATIONS. PRODUCTS FORMALLY ESCC, QML OR JAN QUALIFIED ARE DEEMED SUITABLE FOR USE IN AEROSPACE BY THE CORRESPONDING GOVERNMENTAL AGENCY.

Resale of ST products with provisions different from the statements and/or technical features set forth in this document shall immediately void any warranty granted by ST for the ST product or service described herein and shall not create or extend in any manner whatsoever, any liability of ST.

ST and the ST logo are trademarks or registered trademarks of ST in various countries.

Information in this document supersedes and replaces all information previously supplied.

The ST logo is a registered trademark of STMicroelectronics. All other names are the property of their respective owners.

© 2014 STMicroelectronics - All rights reserved

STMicroelectronics group of companies

Australia - Belgium - Brazil - Canada - China - Czech Republic - Finland - France - Germany - Hong Kong - India - Israel - Italy - Japan - Malaysia - Malta - Morocco - Philippines - Singapore - Spain - Sweden - Switzerland - United Kingdom - United States of America

www.st.com